IOPscience iopscience.iop.org

Home Search Collections Journals About Contact us My IOPscience

Heterojunctions of solid C_{60} and crystalline silicon: rectifying properties and energy-band models

This article has been downloaded from IOPscience. Please scroll down to see the full text article.

1995 J. Phys.: Condens. Matter 7 L201

(http://iopscience.iop.org/0953-8984/7/14/004)

View the table of contents for this issue, or go to the journal homepage for more

Download details:
IP Address: 171.66.16.179
The article was downloaded on 13/05/2010 at 12:52

Please note that terms and conditions apply.

J. Phys.: Condens. Matter 7 (1995) L201–L207. Printed in the UK

LETTER TO THE EDITOR

Heterojunctions of solid C_{60} and crystalline silicon: rectifying properties and energy-band models

K M Chen†, Y Q Jia†, S X Jin†, K Wu†, W B Zhao†, C Y Li†, Z N Gu‡ and X H Zhou‡

† Department of Physics, Peking University, Beijing 100871, People's Republic of China
‡ Department of Chemistry, Peking University, Beijing 100871, People's Republic of China

Received 24 January 1995

Abstract. Heterojunctions of undoped solid C_{60} and n- or p-type-doped crystalline Si have been obtained. Current–voltage measurements show that both C_{60}/n-Si and C_{60}/p-Si contacts are rectifying but their directions of rectification are opposite. Thermal activation measurements at a fixed foward bias show an exponential dependence of current on the reciprocal of temperature, from which we determine the effective barrier height as 0.30 eV for C_{60}/n-Si and 0.48 eV for C_{60}/p-Si. Using energy-band models for heterojunctions we assign values to the positions of the conduction and valence bands of the solid C_{60} relative to those of crystalline Si and derive the electron affinity and band gap of solid C_{60} film as 3.92 eV and <1.72 eV, respectively.

C_{60} and other closed-shell all-carbon molecules (fullerenes) are, owing to their properties, of great scientific interest [1–3]. The success in producing fullerenes in large quantities [4, 5] has given rise to a wide range of experimental work on solid C_{60}. It has been found that alkali-metal-doped solid C_{60} can be superconducting [6], while undoped solid C_{60} films are insulating or semiconducting and show some remarkable electrical and optical properties [7–16]. Recent studies have shown that undoped solid C_{60} film interacts strongly with Si substrate [13–17]. Scanning tunnelling microscopy and scanning tunnelling spectroscopy studies have confirmed that C_{60} molecules form strong bonds with Si substrate, and that this involves a significant charge transfer between C_{60} and Si substrate [17]. However, less is known about the electrical properties of a C_{60}/Si contact. The present article reports on electrical properties of C_{60}/n-Si and C_{60}/p-Si contacts. Strong rectifying behaviour has been observed which is attributed to a potential barrier at the C_{60}/Si interface. Effective barrier heights in the C_{60}/n-Si and C_{60}/p-Si heterojunctions are determined. We propose energy-band models for the heterojunctions from which the values of the electron affinity and band gap of solid C_{60} film are estimated.

In this work, two kinds of sample were prepared: (i) C_{60}/n-Si, with n-type crystalline Si(111) wafers at 30 Ω cm resistivity as the substrate for C_{60} film growth; (ii) C_{60}/p-Si, with p-type *epitaxial Si(111) layers of 2–4 Ω cm resistivity as the substrate. To obtain a good* ohmic contact, gold film (~500 nm) and aluminium film (~1000 nm) were deposited on the back surfaces of the n-Si and p-Si substrates, respectively. The aluminium film deposition was followed by a 30 min annealing at 500 °C in a N_2 atmosphere. The Si wafers were dipped in a HF:H_2O = 1:20 solution to remove any surface oxide, rinsed in deionized water, blown dry with N_2 gas flow, and then immediately transferred to an ultrahigh-vacuum (UHV) chamber for C_{60} deposition. C_{60} powders were prepared by the conventional AC arc method and purified by repeatedly performing liquid chromatography. Evaporation of C_{60} powder

0953-8984/95/140201+07$19.50 © 1995 IOP Publishing Ltd

(99.9% purity) was performed in a Balzers UMS-500 UHV system with a chamber pressure of 10^{-9} Torr and a Si substrate temperature of 200 °C. The deposition rate was ~1 nm min^{-1} and the C_{60} film thickness was monitored *in situ* by a quartz-crystal oscillator. The C_{60} film obtained is polycrystalline with a face-centred cubic structure as revealed by x-ray diffraction pattern measurements. Titanium electrode dots of area 5.03×10^{-3} cm^2 were finally evaporated onto the C_{60} films at 100 °C in the same UHV system. The final thickness of the C_{60} films was determined to be 200 nm by use of a surface profiler (Sloan: Dektak 3030 ST).

Current–voltage (J–V) and current–temperature (J–T) measurements were performed with a HP 34401A multimeter. The Ti/C_{60}/n-Si or Ti/C_{60}/p-Si junction was connected in series to a 1 kΩ resistor so that current could be measured via the potential drop across the resistor. The junction temperature was monitored with a thermocouple placed in contact with a copper sample holder.

Figure 1 shows a typical J–V curve (semilogarithmic plot of current density versus bias voltage) of a Ti/C_{60}/n-Si junction at 280 K. The bias voltage is the voltage on the Ti electrode with respect to the Si substrate. The junction was found to be conducting when the Ti electrode was at a positive bias voltage while the current for a negative bias voltage was much smaller. Thus the Ti/C_{60}/n-Si structure was rectifying. As shown in figure 1, the rectification ratio is greater than 3×10^3 at ±2 V. The log J–V curve is almost linear for forward biases below 0.3 V while the curve bends when the forward bias exceeds about 0.3 V, which can be interpreted as the series resistance effect. We analysed the forward J–V data using

$$J = J_0 \left\{ \exp\left[\frac{q(V - A_e J R_s)}{nkT} \right] - 1 \right\} \tag{1}$$

where J is the current density, V is the potential drop across the sample, A_e is the area of the Ti electrode, R_s is the series resistance of the sample, q is the electron charge, n is the ideality factor, k is Boltzmann's constant, and T is the temperature. In the case of $q(V - A_e J R_s) > 3nkT$ the first derivation of (1) leads to

$$\frac{\mathrm{d}V}{\mathrm{d}J} = A_e R_s + \frac{nkT}{qJ}. \tag{2}$$

At a fixed temperature, R_s- and n-values can be determined by analysing J–V data using (2). For example, at 280 K, we obtained $R_s = 2.0 \times 10^4$ Ω and $n = 3.5$. The high resistance must be due to the undoped C_{60} film and the large n-factor may be due to the importance of interface states at the C_{60}/Si interface.

The inset in figure 1 shows results of thermal activation measurements over a temperature range of 280–330 K. For a given forward bias at 0.5 V ($A_e J R_s \ll 0.5$ V), the plot of $\ln J$ against $1/T$ is a straight line indicating that the current-transport mechanism involves a thermally activated process. After least-squares fitting we found that J_0 in (1) is an exponential function of $1/T$, i.e.

$$J_0 = J_{00} \exp(-q\varphi_{\text{eff}}/kT) \tag{3}$$

where $J_{00} = 1.4 \times 10^5$ $\mu\text{A cm}^{-2}$ and $q\varphi_{\text{eff}} = 0.30$ eV for a C_{60}/n-Si sample. $q\varphi_{\text{eff}}$ denotes the effective barrier height under zero-bias conditions, which is generally related to the energy-band structure of solid C_{60} and Si, the Fermi level in C_{60} and Si, and the C_{60}/Si interface states, as will be discussed later.

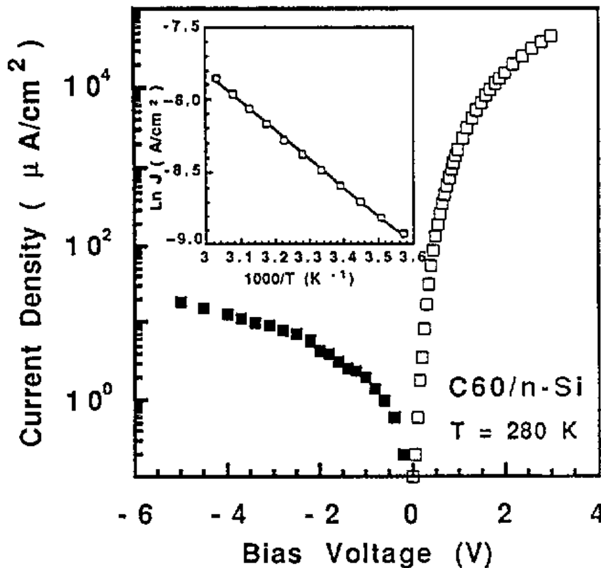

Figure 1. Current–voltage characteristics of a C_{60}/n-Si heterojunction at 280 K. The inset shows data from thermal activation measurements at a fixed forward bias of 0.5 V.

The Ti/C_{60}/p-Si structure was also found to be rectifying but its direction of rectification was opposite to that of Ti/C_{60}/n-Si, i.e. a negative bias applied to the Ti electrode with respect to the Si substrate corresponds to forward conduction. Figure 2 shows a typical J–V curve for Ti/C_{60}/p-Si at 300 K. It can be seen that the rectification ratio is greater than 10^4 at ± 2 V. Analysing the J–V data of figure 2 by use of (2) we find $R_s = 4.7 \times 10^4\ \Omega$ and $n = 2.6$ at $T = 300$ K. The value of the series resistance of the Ti/C_{60}/p-Si junction is near that of the Ti/C_{60}/n-Si junction while the n-factor is better in Ti/C_{60}/p-Si than in Ti/C_{60}/n-Si. The inset in figure 2 shows the J–T results for the Ti/C_{60}/p-Si sample at a fixed forward bias of -0.5 V. Fitting the data to (3), the value of $q\varphi_{\text{eff}}$ is found to be 0.48 eV for the C_{60}/p-Si sample.

To confirm that the rectifying effect is not due to a potential barrier at the Ti/C_{60} interface, we have measured control samples of Ti/C_{60}/Ti structure and found a linear J–V relation indicating that the Ti/C_{60} contact is ohmic. The fact that Ti/C_{60}/n-Si and Ti/C_{60}/p-Si have opposite directions of rectification implies that there are potential barriers preventing electron and hole diffusion at the C_{60}/n-Si and C_{60}/p-Si interfaces, respectively. In order to explain the potential barrier formation in the C_{60}/Si heterojunction we introduce energy-band models as shown in figure 3. Figure 3(a) gives the energy-band diagram for undoped solid C_{60} and n-Si before their contact. The subscript 1 denotes C_{60} while subscript 2 denotes Si. χ, $q\varphi_m$, and E_g represent the electron affinity, work-function, and band gap, respectively. E_{vac} is the vacuum level. E_c, E_v, E_F represent the bottom of the conduction band, the top of the valence band, and the Fermi level, respectively. ΔE_c represents the difference in energy between the conduction-band edges of solid C_{60} and Si, and ΔE_v, that between the valence-band edges. Before contact, as is confirmed by the direction of rectification of the C_{60}/n-Si heterojunction, the Fermi level in n-Si, E_{F2}, must be higher than that in solid C_{60}, E_{F1}. Figure 3(b) shows the energy-band profile for an ideal C_{60}/n-Si heterojunction (in the absence of interface states) at thermal equilibrium. qV_b represents the built-in potential. The sum of qV_{b1} and qV_{b2}, $q(V_{b1} + V_{b2})$, corresponds to the Fermi

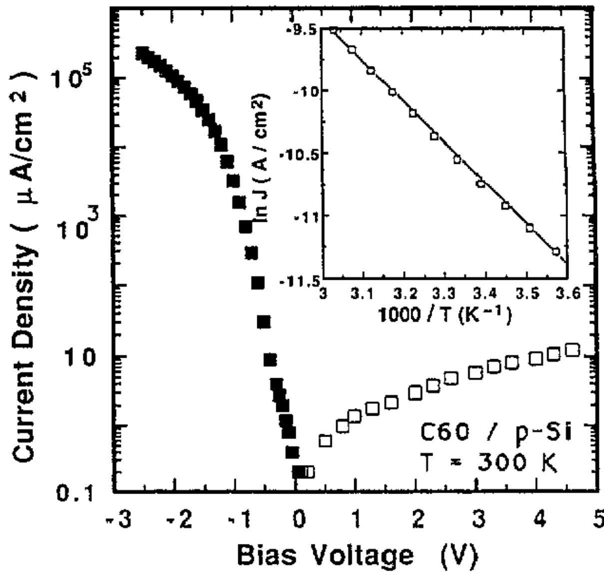

Figure 2. Current–voltage characteristics of a C_{60}/p-Si heterojunction at 300 K. The inset shows data from thermal activation measurements at a fixed forward bias of −0.5 V.

level difference, $E_{F2} - E_{F1}$, before contact. Interface states may be introduced due to lattice mismatch and impurities at the C_{60}/Si interface (we have observed interface state density as high as around 10^{12}–10^{13} eV^{-1} cm^{-2} from capacitance transient measurements but detailed results will be given elsewhere). The interface states can trap electrons from the solid C_{60} and Si sides to make the interface negatively charged and modify the energy-band structure of the C_{60}/n-Si heterojunction as shown in figure 3(c). It can be seen from figure 3(c) that conduction-band electrons transferring from n-Si to C_{60} need to overcome a barrier of $q\varphi_{\text{eff}} = (\Delta E_c + qV_{b2})$, which is the so-called effective barrier height in (2). This barrier can be reduced under forward bias and increased under reverse bias, thus providing an interpretation of the observed rectification in the C_{60}/n-Si heterojunction. Figure 3(d) shows the energy-band diagram for the C_{60}/p-Si heterojunction in thermal equilibrium. It can be seen that valence-band holes transferring from Si to C_{60} must overcome a barrier of $q\varphi_{\text{eff}} = \Delta E_v + q(V_{b1} + V_{b2})$. When a negative bias is applied to the C_{60} side with respect to the p-Si side the effective barrier is reduced and the junction is forward conducting.

The value of V_{b2} can be obtained from measurements of the high-frequency capacitance of the C_{60}/Si junction. Capacitance–voltage (C–V) measurements wee performed with a high-frequency (1 MHz) Model 410 C–V plotter. The total capacitance of the junction is a series combination of the depletion-layer capacitance of C_{60} and that of Si, i.e.

$$1/C = 1/C_{C_{60}} + 1/C_{\text{Si}}. \tag{4}$$

In our sample the C_{60} layer was very thin (200 nm), so the whole layer must be depleted. Hence, $C_{C_{60}}$ can be given by

$$C_{C_{60}} = A_e \varepsilon_{C_{60}} \varepsilon_0 / d_{C_{60}} \tag{5}$$

where $d_{C_{60}}$ is the thickness of the C_{60} layer and ε_0 is the permittivity in vacuum. Recent studies have given the value of $\varepsilon_{C_{60}}$ as 3.7±0.1 [13]. Thus from (4) and inserting our values

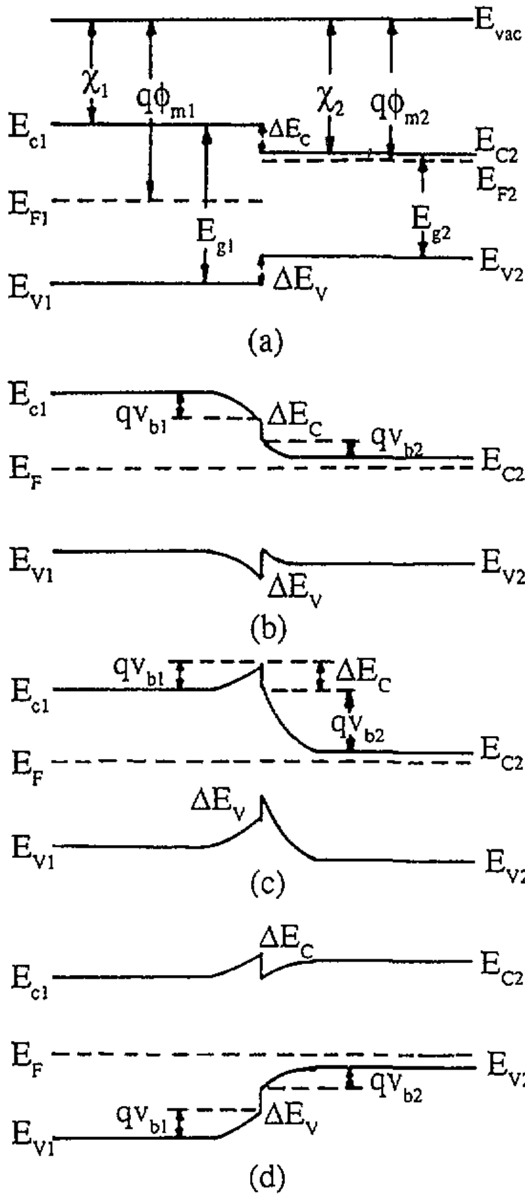

Figure 3. Energy-band models for C_{60}/Si heterojunctions: (a) before the C_{60}/n-Si contact; (b) ideal contact of C_{60}/n-Si without interface states; (c) the C_{60}/n-Si contact with interface states; (d) the C_{60}/p-Si contact with interface states.

for $D_{C_{60}}$ and A_e, $C_{C_{60}}$ is found to be 82.4 pF. C_{Si} is determined by the surface potential ψ_s (V_{b2} corresponds to ψ_s at zero-bias conditions) [18]. For a p-type semiconductor, if the minority carriers are neglected, C_{Si} can be given as

$$C_{Si} = A_e \varepsilon_{Si} \varepsilon_0 \left[1 - \exp(-\beta\psi_s)\right] / \left\{\sqrt{2} L_D F(\beta\psi_s)\right\} \tag{6}$$

where

$$F(\beta\psi_s) = [\exp(-\beta\psi_s) + \beta\psi_s - 1]^{1/2} \tag{7}$$

and

$$L_D = (\varepsilon_{Si}\varepsilon_0 kT/N_A q^2)^{1/2}. \tag{8}$$

L_D is Debye's screening length, $\beta = q/kT$, and N_A is the shallow acceptor density in p-Si. From high-frequency C–V measurements we obtain 6.8×10^{15} cm^{-3} for the shallow acceptor density in p-Si and 74.5 pF for the zero-bias capacitance of the Ti/C_{60}/p-Si sample. From these values and the value of $C_{C_{60}}$ we calculated V_{b2} from (4) and (6)–(8) obtaining $qV_{b2} = 0.01$ eV for the Ti/C_{60}/p-Si sample. In a similar way, for the Ti/C_{60}/n-Si sample, the shallow donor density in n-Si was found to be 5.1×10^{13} cm^{-3}, the zero-bias capacitance was 19.9 pF, and $qV_{b2} = 0.17$ eV.

Using the results we can define the positions of solid C_{60} energy bands relative to those of crystalline bulk Si. As qV_{b2} and $q\varphi_{eff}$ for C_{60}/n-Si are 0.17 and 0.30 eV, respectively, we get $\Delta E_c = 0.13$ eV, i.e. the discontinuity in conduction-band edges is 0.13 eV. Furthermore, the electron affinity of solid C_{60} is $\chi_1 = \chi_2 - \Delta E_c = 3.92$ eV, where the electron affinity of bulk Si, χ_2, is taken as 4.05 eV. As for C_{60}/p-Si, $qV_{b2} = 0.01$ eV and $q\varphi_{eff} = 0.48$ eV, it can be deduced that $\Delta E_v < 0.47$ eV and $E_{g1} < 1.72$ eV (the band gap of bulk Si at 300 K is taken as 1.12 eV).

The value of 3.92 eV for the electron affinity of solid C_{60} is obtained, for the first time, from electrical measurements on a C_{60}/Si heterojunction. This value may be compared with the reported value of 2.6–2.8 eV from a UV photoemission study of negatively charged C_{60} ions [19] but the polarization screening value of 0.7 eV [20] should be added. The band-gap value of <1.72 eV for solid C_{60} is in good agreement with the value of 1.7 eV measured in a photoconductance experiment on solid C_{60} films [12] and the value of 1.64 eV obtained from fitting the optical absorption data of solid C_{60} film to an equation used for amorphous semiconductors [21], but different from those values given by electron energy-loss spectroscopy (1.8 eV) [22], XPS (1.9 eV) [23], and ellipsometric measurements (2.3 eV) [24] for solid C_{60}.

In summary, we have found that both C_{60}/n-Si and C_{60}/p-Si contacts are rectifying, and interpreted their J–V and J–T behaviour using energy-band models. Electrical measurements have enabled us to define the positions of the conduction and valence bands of solid C_{60} relative to those of crystalline Si and estimate values for the electron affinity and band gap of solid C_{60}. Further investigation of the current-transport mechanism and C_{60}/Si interface states in C_{60}/Si heterojunctions is under way.

We thank M X Xing for experimental assistance. We are also grateful to Professor R S Han and Professor A Rhys for many valuable discussions.

References

[1] Kroto H W, Heath J R, O'Brien S C, Curl R F and Smalley R E 1985 *Nature* **318** 162
[2] Curl R F and Smalley R E 1988 *Science* **242** 1017
[3] Haddon R C, Hebard A F, Rosseinsky M J, Murphy D W, Duclos S J, Lyons K B, Miller B, Hosamilia J M, Fleming R M, Kortan A R, Glarum S H, Makhija A V, Muller A J, Eick R H, Zahurak S M, Tycko R, Dabbagh G and Thiel F A 1991 *Nature* **350** 320
[4] Kratschmer W, Fostiropoulos K and Huffman D R 1990 *Chem. Phys. Lett.* **170** 167
[5] Kratschmer W, Lamb L D, Fostiropoulos K and Huffman D R 1990 *Nature* **347** 354

[6] Hebard A F, Rosseinsky M J, Haddon R C, Murphy D W, Glarum S H, Palstra T T M, Hamirez A P and Kortan A R 1991 *Nature* **350** 600

[7] Mort J, Ziolo R, Machonkin M, Huffman D R and Ferguson M I 1991 *Chem. Phys. Lett.* **186** 284

[8] Kaiser M 1992 *Solid State Commun.* **81** 261

[9] Mort J, Okamura K, Machonkin M, Ziolo R, Huffman D R and Ferguson M I 1991 *Chem. Phys. Lett.* **186** 281

[10] Pichler K, Graham S, Gelsen O M, Friend R H, Romanow W J, McCauley J P Jr, Coustel N, Fischer J E and Smith A B III 1991 *J. Phys.: Condens. Matter* **3** 9259

[11] Yonehara H and Pac C 1992 *Appl. Phys. Lett.* **61** 575

[12] Hosoya M, Ichimura K, Wang Z H, Dresselhaus G, Dresselhaus M S and Eklund P G 1994 *Phys. Rev.* B **49** 4981

[13] Chen K M, Jia Y Q, Jin S X, Wu K, Zhao W B, Li C Y and Gu Z N 1994 *J. Phys.: Condens. Matter* **6** L367

[14] Chen K M, Jin S X, Jia Y Q, Wu K, Li C Y, Zhou X H and Gu Z N 1995 *Chin. J. Semicond.* at press

[15] Pichler K, Harrison M G, Friend R H and Pekker S 1993 *Synth. Met.* **55–57** 3229

[16] Maruno S, Inanaga K and Isu T 1993 *Appl. Phys. Lett.* **63** 1339

[17] Wang X D, Hashizume T, Shinohara H, Saito Y, Nishina Y and Sakurai T 1993 *Phys. Rev.* B **47** 15923

[18] Sze S M 1981 *Physics of Semiconductor Devices* (New York: Wiley) p 362

[19] Yang S H, Pettiette C L, Conceicao J, Cheshnovsky O and Smalley R E 1987 *Chem. Phys. Lett.* **139** 233

[20] Lof R W, van Veenendaal M A, Koopmans B, Jonkman H T and Sawatzky G A 1992 *Phys. Rev. Lett.* **68** 3924

[21] Skumanuch A 1991 *Chem. Phys. Lett.* **182** 486

[22] Hansen P L, Fallon P J and Kratschmer W 1991 *Chem. Phys. Lett.* **181** 367

[23] Weaver J H, Martins J L, Komeda T, Chen Y, Ohno T R, Kroll G H, Troullier N, Haufler R E and Smalley R E 1991 *Phys. Rev. Lett.* **66** 1741

[24] Ren S L, Wang Y, Rao A M, McRae E, Holden J M, Hager T, Wang Kaian, Lee Wen-Tse, Ji H F, Selegue J and Eklund P C 1991 *Appl. Phys. Lett.* **59** 2678